Goddard
IN-89-CR
237055
19P.

FINAL TECHNICAL REPORT

GRANT NAG 5-1020

Submitted to NASA on November 2, 1989

UV Observations of NGC 205

Eric M. Wilcots, Paul W. Hodge, Paul B. Eskridge

Erika Böhm-Vitense, and Francesco Bertola

(NASA-CR-185975) UV OBSERVATIONS OF NGC 205 Final Report (Washington Univ.) ~~19 p~~ 20 p CSCL 03A

N90-11661
54 7192
Unclas
G3/89 0237055

November 1, 1989

INTERIM STATUS REPORT

NASA GRANT NAG 5-1020

UV Observations of NGC 205

Eric M. Wilcots, Paul W. Hodge, Paul B. Eskridge

Erika Böhm-Vitense, and Francesco Bertola

Abstract

Low-resolution IUE observations of the dwarf elliptical galaxy NGC 205 show that the UV spectral energy distribution (SED) of the galaxy is relatively flat. Spectra centered on the nucleus and on a region north of the nucleus show evidence of recent "bursts" of star formation which contribute strongly to the UV spectral energy distribution. We fit the UV spectra with a composite spectrum based on a Miller-Scalo initial mass function, an underlying older population (modelled using the UV spectrum of 47 Tuc), and an extinction based on a SMC-like extinction curve. This fit implies that the total mass of young stars (with $M \geq 1M_\odot$) in the galaxy is $\sim 7\times10^5 M_\odot$, which can be compared to the total mass of globular cluster like stars in the galaxy of $\sim 8\times10^7 M_\odot$.

I. Introduction

NGC 205, a dwarf elliptical companion of M31, is a good example of a star forming dwarf elliptical galaxy. Nearly forty years ago Baade (1951) detected several O and B stars, as well as a significant amount of dust, in its central region. Hodge (1973a, hereafter H73) measured surface brightnesses and colors in the galaxy, mapped the dust clouds and measured magnitudes for the luminous blue stars. Price and Grasdalen's (1983) surface photometry determined that the dust clouds have properties similar to those of Galactic clouds. VLA observations of NGC 205 (Johnson and Gottesman 1983) showed that HI gas is roughly aligned with the dust and young stellar population of the galaxy and amounts to a few times $10^5 M_{\odot}$. Gallagher and Mould (1981), Mould *et al.*(1984), and Richer *et al.*(1984) found evidence for a significant intermediate age population within NGC 205, at least in the outer parts of the galaxy. Richer *et al.*(1984) identified several possible carbon stars and reached the conclusion that the galaxy is experiencing a small burst after a period of relatively constant star formation. On the basis of its overall population, Kormendy (1985) placed NGC 205 on the same physical sequence as the Sculptor-type dwarfs.

In this contribution we use UV observations of two areas in the central region of NGC 205 to fit the observed ultraviolet spectral energy distribution (SED) to a composite model spectrum. As noted by Burstein *et al.*(1989), the SED of NGC 205 is relatively flat, a phenomenon that is not uncharacteristic of some early type galaxies. The flatness of the SED can be explained by the excess UV contribution at short wavelengths from the newly formed blue stars, and in our models we examine the effects of different initial mass functions (IMF). Secondly, there is a strong contribution to the mid-UV (2500-3000 Å) from the underlying, older population of stars. We chose to model this component by using the observed UV spectrum of a globular cluster. Finally, the UV SED of the galaxy will be affected by the extinction caused by the dust and we compare the extinction curves resulting from studies of the SMC (Fitzpatrick and Savage 1982, Nandy 1984) and the Galaxy (Savage and Mathis 1981), and apply them to NGC 205.

In the following section we discuss our observations and reductions. In section II we also present and discuss the spectral energy distribution of NGC 205, and in section III we describe the spectral synthesis of our model and present the results. We give our conclusions in section IV.

II. Observations and Data

a. Observations

We used the IUE telescope to obtain eight UV spectra (Table 1), including two that spanned the US-European shifts, allowing longer exposures than would otherwise be possible. Two regions in NGC 205 were observed: the nuclear area and "Region B", which is about one arc minute north of the nucleus in part of the main body of the galaxy that has some resolved blue stars and dust (Fig. 1). The coordinates of region B are $\alpha = 00h37m38.6s$, and $\delta = +41^{\circ}25'08'$ (1950), as measured by off-set from field star SAO 036570. The aperature of the spectrograph is 10×20 arcsec (Fig. 1), and thus it accepts light from a moderately large region of the galaxy in each case. The spectra are weak and the average signal-to-noise ratio we obtained is ~ 3. Spectral features were difficult to distinguish, but the spectral energy distribution is measurable and a few spectral lines are detectable.

b. Spectral Energy Distribution

In Figure 2 we present the SED for each of the two regions and in each wavelength range. The distributions were obtained by averaging the detected flux over 35 Åbins in the short wavelength region and 50 Åbins in the long wavelength region. The short wavelength SED's have been cut longward of the Lyman-α line to avoid contamination from that feature. The SED's have also been corrected for the Galactic foreground extinction assuming $E(B-V) = 0.14$ (Burstein and Heiles 1984) and the Seaton (1979) extinction law. The most obvious feature of our SED's is that they are essentially flat or slightly rising to the blue for both regions in NGC 205, a characteristic of star-forming elliptical galaxies (Burstein *et al.*1989).

c. Spectral Features

Identification of spectral features in the IUE spectra is an important step towards a determination of the contribution from different components. Given the quality of our spectra, the most important lines in this determination are the Mg II lines around 2800 Å - which are very prominent in the spectra of many globular clusters - and the Fe II line near 2580 Å, which is prominent in the spectra of B stars (Wu *et al.*1983)

III. The Model

In modelling the spectra we employ a technique that bears some resemblance to the efforts of many authors (Fanelli *et al.*1987, Fanelli *et al.*1988, Pickles 1985, and references therein) who have modelled the composite spectra of early-type galaxies. We combine the limited information from the detected spectral lines with the similarly limited information that comes from the SED. Following Bica (1987), who used the integrated spectra of star clusters to model the SED of galactic nuclei, we will use the integrated spectrum of a globular cluster to model the older population in NGC 205. We have compiled an integrated spectrum one would expect to find from a single burst of star-formation that follows a particular initial mass function. The final ingredient in our model is the effect of the internal extinction of NGC 205.

The UV excess detected in the spectra of many late type galaxies has been explained using a variety of mechanisms. Hodge (1973b) and others (e.g. Bruzual 1983 and Burstein *et al.*1989) have suggested that O and B giant stars may account for the "UV rising branch" seen in both dwarf and giant elliptical galaxies. Other authors (most notably Nesci and Perola 1985) have suggested that blue HB stars explain the UV excess and, more recently, Bertelli *et al.*(1989) proposed that post-asymptotic giant branch stars are responsible. Because O and B stars are seen in NGC 205 and because it is probably too metal rich for its UV SED to be affected by PAGB stars, we assume that the UV excess in this galaxy is largely due to the young stars.

a. Population II Contribution

In determining the Population II contribution to the SED of NGC 205 we look first at the metallicity and color of peripheral regions of the galaxy. Our working assumption is that the older population can be accurately modelled by using the spectrum of an appropriate globular cluster. For the metallicity we use the approximate value of $[M/H] \sim -0.85 \pm 0.2$ as determined by Mould *et al.*(1984). H73 found that the (B-V) color of NGC 205 varied from 0.52 in the center to 0.82 when outer regions were included in the aperature. We adopt the colors of the outer regions for the purpose of understanding the Population II contribution. It should be noted, however, that because we do not know the star-forming history of NGC 205 we cannot be certain that the 'old' population in the nucleus is similar to the 'old' population in the rest of the galaxy. Among the well-studied Galactic globular clusters, 47 Tuc (NGC 104) is seen as the prototypical metal-rich cluster (Hesser *et al.*1987). It has a metallicity of −0.44 and a color of (B-V)=0.89 (Harris and Racine 1979), which are similar to our adopted values for NGC 205, although 47 Tuc has a slightly higher metallicity than NGC 205. Despite this we find that 47 Tuc is the most appropriate Galactic globular cluster with data available for use in modelling the old star contribution to the UV SED of NGC 205.

We show in Figure 3 the IUE archive spectra of 47 Tuc. The data have been corrected for galactic foreground extinction using the extinction curve described by Seaton (1979) (cf. section IIIc.) and an E(B-V) value of 0.04 towards 47 Tuc (Harris and Racine 1979). The spectra of 47 Tuc have also been corrected to the apparent distance modulus of NGC 205 which we take to be 24.7 (H73). The two most notable features seen in Figure 3 are the Mg II lines around λ2800Å and the sharp increase in the continuum towards 3500Å. Both of these features prove important [illegible] models.

In Figure 4 we show the discernable spectral features in our IUE spectra for the nucleus and Region B, respectively. In the nucleus we have identified two features, the first of which is a blend of the two Mg II lines at 2795.5Å and 2802.7Å, and the second of which is the Mg I line at 2852.1Å (Cardelli and Bohm-Vitense 1982). Both features are prominent in the spectrum of 47 Tuc. Unfortunately, the Mg II lines in our spectrum are severely blended making it impossible to use their relative strengths to constrain the contribution from the globular-like population. The 2852Å Mg I feature, however, indicates the presence of a strong 47 Tuc-like population.

For region B the picture is not quite so clear. As shown in Figure 4b, there are several possible spectral features present in our spectrum, although only the Fe II line at 2583Å can be positively identified, and it is most likely saturated. This line is prominent in the spectra of late O and early B type giants (Wu *et al.*1989) indicating that the Population I component is much stronger in region B than in the nucleus. Although other features - at apparent wavelengths 2748Å and 2784Å - are tantilizingly close to identified lines (Mn II at 2740Å and Mg II at 2795Å respectively), we are hesistant to draw any conclusions from them. We are unable to identify the apparent bump centered at 2705Å.

Our second means of constraining the contribution from the globular-like population is by determining the apparent flux observed in the near-UV wavelengths. We expect the contribution from this population to be most important longward of λ2500Å, especially considering the sharp rise in the continuum of 47 Tuc near this wavelength. Assuming the 47 Tuc energy distribution will dominate at these wavelengths, we estimate that we are observing the integrated UV light of the equivalent of a few hundred times the distance - corrected flux contained within the IUE aperature on 47 Tuc (it will be our convetion throughout to refer to the Population II contribution in terms of flux of 47 Tuc contained within the IUE aperature). In correcting for the distance we adopted μ_{47Tuc}~13.46 (Harris and Racine, 1979), and μ_{N205}~24.7 (H73). We reached a similar conclusion by comparing the surface brightness of NGC 205 in the U,B and V bands (H73) with the observed brightness of 47 Tuc (Illingworth and Illingworth 1976, Hesser *et al.*1987).

b Population I Contribution Young Stars

Baade (1951) originally estimated that there were a dozen blue OB stars located in the central parts of NGC205. Later, H73 detected more than 40 such stars on Baade's original plates down to a limiting magnitude of ~ 21. For our purposes we are concerned only with the blue stars that are visible in the area covered by the IUE aperature. The exact pointing and orientation of the IUE aperature were determined and compared to a print of Baade's deep blue plate that was used by H73. Independent counts of the number of stars in the IUE slits for the nucleus and region B were made by two of the authors (PH and PBE), and were found to agree fairly well (cf. Table II). H73 showed that the limiting magnitude of the plate was $B \sim 21.0$, which corresponds (given the foreground extinction and distance modulus) to a limiting absolute magnitude of $M_B \sim -3.7$. The B-magnitude of the brightest star was found to be $M_B \sim -5.3$ (H73).

Gallagher and Mould (1981) have argued, based in part on the lack of observed M supergiants, that the resolved blue stars are evolved supergiants and that the brightest blue star visible has a mass of ~ $9M_\odot$. We estimate, based on the evolutionary tracks of Maeder and Meynet (1987), that the blue stars resolved on the photographic plates correspond to initial main sequence masses between ~ $20M_\odot$ and ~ $10M_\odot$, although this is quite uncertain. The implication of either estimation is that NGC 205 has recently (i.e. in the past ~ 10^7 years) undergone a period of star formation. Gallagher and Mould determined the age of the 'burst' to be ~ $2\times10^7 yrs$. Such a burst will also have resulted in the formation of a large number of lower-mass stars that will collectively have a significant effect on the SED of the galaxy. To model the complete effect of the Population I component on the SED it is necessary to make some assumptions about the IMF.

We assume that the young population in NGC 205 can be described by the Miller-Scalo (1979) IMF. We use the counts of the number of massive stars present within the IUE aperature - detailed above - to normalize the IMF. Given this normalization we then compute the total number of stars expected from a single burst of star formation, down to a lower limit of $1M_\odot$. Extending the IMF below $1M_\odot$ does not significantly effect the ultraviolet SED of the subsequent integrated spectrum. Since the IMF gives us the number of stars in a given mass bin we have identified each bin with a certain spectral type, using $2M_\odot$ bins down to $4.5M_\odot$ and then $1M_\odot$ bins for the lower masses. The mean spectral type for each bin was determined and corresponding stellar spectra from the IUE archives were adopted (Wu *et al.*, 1983). After correcting for foreground reddening and distance, the individual stellar spectra were then scaled by the appropriate factors for the IMF and were summed using 2Å bins with a linear interpolation between bins. The integrated spectra were scaled to the distance modulus of NGC 205 ($\mu = 24.7$) and then corrected for Galactic foreground extinction.

The integrated spectra resulting from the calculated IMFs are very dependent on the initial assumption about the nature of the luminous blue stars. To illustrate this we show the integrated spectra resulting from a single burst of star formation that can be described by the Miller-Scalo IMF. In Figure 5 we present the IMF normalized with 14 stars between 16 and 32 $M_\odot$ (solid line) and normalized with the same number of stars between 10 and 20 $M_\odot$ (dashed line). It has become evident from a number of studies (Humphreys 1979a,b, Böhm-Vitense *et al.*1984, and Gallagher and Mould 1984) that the bright blue stars in young systems are typically evolved, so we will use the IMF plotted in Figure 5b. We have also adopted the assumption that the Miller-Scalo IMF is more appropriate for other galaxies than the Salpeter IMF (Humphreys and Blaha 1989, Massey *et al.*1989, Kennicutt 1989), although this is somewhat uncertain.

c. *Internal Extinction in NGC 205*

Nandy (1984) has shown that the ultraviolet extinction curves for the Large and Small Magellanic Clouds are significantly different from the Galactic case (Mathis 1987), with the SMC law being the most different. Specifically, the SMC extinction curve rises more steeply towards shorter wavelengths than either the LMC or Galactic curves. Secondly, the 2175Å bump, while prominent in the Galactic extinction curve, is not present in the SMC curve. While the differences are subtle at wavelengths longward of the λ2175Å feature, there are significant differences between them at and shortward of the 'bump', implying that the shape and characteristics of a galaxy's extinction curve is a function of the galaxy's metallicity.

The final ingredient of our model is the reddening internal to NGC 205, and this is, unfortunately, poorly determined. There are several means by which we can constrain the reddening component. The first is to assume a particular reddening law and an accurate measurement of the value of E(B-V) for the galaxy, and then calculate the amount of extinction at any given wavelength. This method is a function of the other parameters of the model, and, therefore, does not provide a stringent constraint. Secondly, we can hope to detect the effects of the 2175Å bump in our observations and thereby constrain the reddening law.

We examine this second possibility first. The observed flux we find at and around 2175Å should give us a measure of the strength of the 'bump' in NGC 205, and it was our initial hope to be able to determine the internal extinction with this measurement. We found, however, that the level of noise in the data only allows us to determine a *lower limit* on the amount of extinction that would have to be there for us to detect it. By comparing the observed fluxes both longward and shortward of the the 'bump' with the flux at 2175Å, we conclude that there would have to be an equivalent of at least 0.44 magnitudes of extinction at 2175Å for the bump to be detectable in our spectra. If we were to assume a Galactic reddening law, the corresponding value of E(B-V) is no greater than $\sim$ 0.16, which is entirely consistent with other estimations of the reddening, such as by Mould *et al.*(1984) determined E(B-V) to be 0.06 ± 0.02. If we assume that the extinction curve determined for the SMC (Nandy, 1984) is applicable to NGC 205 (due to the relative similarities in their metallicities), we are still unable to draw a more definitive conclusion, as the SMC curve has no 2175Å feature.

d. *Putting It All Together*

Optical inspection of NGC 205 indicate that our region B contains a higher concentration of bright blue stars and associated dust. We have seen in our spectra that the Fe II line at λ2580Å is prominent in region B, further indicating the relative strength of the Population I contribution. In Figure 6a-d we show our modelled SED for region B compared to the observed SED. The parameters of this model are given in Table III, and are discussed below. Taking the observed flux around 2950Å (chosen arbitrarily) in NGC 205 compared to the flux at that wavelength in a distance-corrected spectrum of 47 Tuc, we determined the ratio of those fluxes to be ~ 300. For the young star component we normalize the Miller-Scale IMF to include 10 supergiants between 10 and 20 $M_\odot$, and used the resulting integrated spectrum in the model. We adopt the reddening law of the Small Magellanic Cloud (Nandy 1984) for reasons detailed above, and use an $E(B-V) = 0.10$. The results are shown in Figures 6c and 6d.

The nucleus does not show the prominent signs of young stars that region B does, and we have scaled back the Population I component appropriately. Counts of the brightest blue stars led us to normalize the IMF to include 7 supergiants between 10 and 20 $M_\odot$. The Population II component is stronger in the nucleus than in region B, as can be seen by determining the flux observed near 2950Å. We have, accordingly, fit 400 equivalent 47 Tucs into our model spectrum. Optical evidence shows that the interstellar dust is less prominent at the nucleus compared to region B, and although we employ the SMC extinction curves and a mean E(B-V) of 0.04 for the nucleus. These parameters are also given in Table III, and the results of the fit to the nuclear SED are presented in Figures 6a and 6b.

IV. Discussion

As is generally the case with modelling spectra to fit a set of observations, our results are not unique. The parameters we have listed in Table III are designated to be the best fit not only because they fit the data within reasonable limits, but also because they seem the most reasonable given other evidence. Changing any one parameter drastically will effect the derived fit, but subtle changes will not. In the following paragraphs we examine the effects altering the parameters have on the model SED.

a. Internal Extinction

Interchanging a Galactic extinction curve like that proposed by Seaton will have a serious effect. Because the SMC curve is so steeply sloped at the shorter wavelengths, for a given E(B-V) it provides a factor of 2 or 3 higher extinction - that is the observed flux is then a factor of 2 or 3 reduced from the flux obtained using a Galactic reddening. This difference is particularly noticeable below 2100Å; longward of that the extinction curves are very similar. We have determined the reddening values to be ~ 0.04 for the nucleus and ~ 0.10 for region B. Both values are probably good to within a factor of two; for example, increasing the reddening in the nucleus to 0.12 noticeably alters the fit.

b. Population II Contribution

In the case of region B the Population II component of the synthesis is constrained to within a factor of 2. If we were to include the equivalent of only 150 clusters, for example, we could not account for all the observed flux near 3000Å without drastically increasing the strength of the Population I component to a value entirely inconsistent with our observations shortward of 2000Å. Similarly, increasing the input of globular clusters to 600 would would lead us to equally unreasonable conclusions at 3000Å. The value we have chosen (300 clusters) is consistent with the surface brightness of NGC 205 as determined by H73 and of 47 Tuc (Illingworth and Illingworth 1976).

Our fit for the nucleus has a similar degree of certainty. We have adopted a fit of 400 globular clusters for our integrated spectrum, a value that is not inconsistent with estimates one derives from considering the V band surface brightnesses of both 47 Tuc and NGC 205. Increasing this number much above 400 leaves us with a dramatic excess of near-UV flux, regardless of the value of the other parameters. The observed SED near 3000Å cannot be accounted for with a much weaker Population II contribution.

c. Population I Contribution

We have made two major assumptions about the young star contribution to the UV SED of NGC 205: that it is described by a Miller - Scale IMF; and that the bright, blue objects are evolved giants rather than main sequence stars. Both assumptions are based, in part, upon general characteristics of other galactic systems. If we were to use the Salpeter IMF and leave the other conditions unchanged we see very little difference in the fit of our synthesized model. In other words we cannot, based solely on the examination of the SED, distinguish between the

Salpeter and Miller - Scalo initial mass functions. We can, however, determine the evolutionary status of the luminous blue stars with some degree of certainty. Under the assumption that the lumious blue stars are main sequence stars we would be forced to consider the possibilty that there were only a handful of such stars ($\sim$ 3) in the IUE aperature, a factor of 3 to 5 fewer than have been counted. The assumption that we are seeing evolved stars leads us to more reasonable conclusions. There is possible uncertainty in our estimation of the upper mass range of the IMF. Our determination of the magnitude limit of the photographic plates are accurate only to within $\sim$ 0.3 magnitudes, which translates to an uncertainty of $\sim$ $2.0 M_\odot$ in our upper mass range. If we have overestimated the extent of the mass range represented by the range of blue magnitudes of the stars on the plates, we will have underestimated the number of intermediate mass stars in the IMF. A second uncertainty is in our estimate of how many evolved supergiants fall within our upper mass range. Given that the data is noisiest in the spectral region most influenced by the number of luminous blue stars, our estimate of the number of stars between 10 and 20 $M_\odot$, is good only to within $\sim$ 30%.

d. Mass Determinations

Given the parameters of the adopted IMF, we determined the total mass of Population I stars to be $\sim 2\times10^5 M_\odot$ in region B and $\sim 1\times10^5 M_\odot$ in the nucleus. These regions combine to represent $\sim$ 40% of the total light contributed by the OB-star array (H73). Thus, we conclude that there is a population of $\sim 7\times10^5 M_\odot$ of recently formed stars in NGC 205. This estimate does not include any contribution from young stars with masses $< 1M_\odot$. If we were to extend the Miller - Scalo IMF below $1M_\odot$ we would find an additional $\sim 10^4 M_\odot$ of Population I stars.

From the surface brightness estimates for the nuclear region of 47 Tuc we have determined that there are $\sim 5\times10^4 M_\odot$ of stars within the IUE aperature. Our model leads us to conclude that there are $\sim 4\times10^5 M_\odot$ worth of Population II stars in the two regions combined

V. Conclusion

We have presented model spectra to fit the UV SED for the dwarf elliptical galaxy NGC 205, accounting for the Population I and II contributions as well as the effect of internal reddening. The other unknowns are the shape of the IMF and the reddening law, and the nature of the older stellar population. We have determined, with some uncertainty, that the young stellar population is best described by the Miller-Scalo IMF with the condition that the brightest blue stars visible on the photographic plates have evolved off of the main sequence. Within the IUE aperature there are 10 such stars in region B and 7 such supergiants in the nucleus. The Population II contribution is best fit by using the spectrum of 47 Tuc. We find the equivalent of $\sim$ 300 47 Tucs in region B and $\sim$ 400 such clusters in the nucleus. Finally, we have fit our model assuming an SMC-like extinction law for NGC 205 with a value of E(B-V) of $\sim$0.10 for region B and $\sim$0.04 for the nucleus.

Ackowledgements

We would like to thanks Don Boggs for many helpful discussions. The IUE observations were supported by NASA Grant NAG-5-1020. EMW was kindly supported by NASA Grant NGT-70050.

Table 1.
IUE Spectra of NGC 205

Image	Exposure (min)	Observer
	Nucleus	
LWR 16363	409	Buson
SWP 10314	420	Bianchini
SWP 27023	328	Böhm-Vitense
LWP 7051	370	Böhm-Vitense
	Region B	
LWR 17019	270	Hodge
SWP 21605	210	Hodge
LWP 7051	710	Böhm-Vitense
SWP 27036	697	Böhm-Vitense

Table 2.

Counts of Luminous Blue Stars

Counter	Region B SW	Region B LW	Nucleus SW	Nucleus LW
PBE	7	7	4	4
PH	11	11	6	7
mean	9	9	5	5

Table 3.

Parameters of the Modelled SEDs

Component	Value
Nucleus	
Population I (47 Tuc)	400
IMF	Miller-Scalo
Normalizing number of LBS	7
Extinction Curve	SMC
E(B-V)	0.04
Region B	
Population I (47 Tuc)	300
IMF	Miller-Scalo
Normalizing number of LBS	10
Extinction Curve	SMC
E(B-V)	0.10

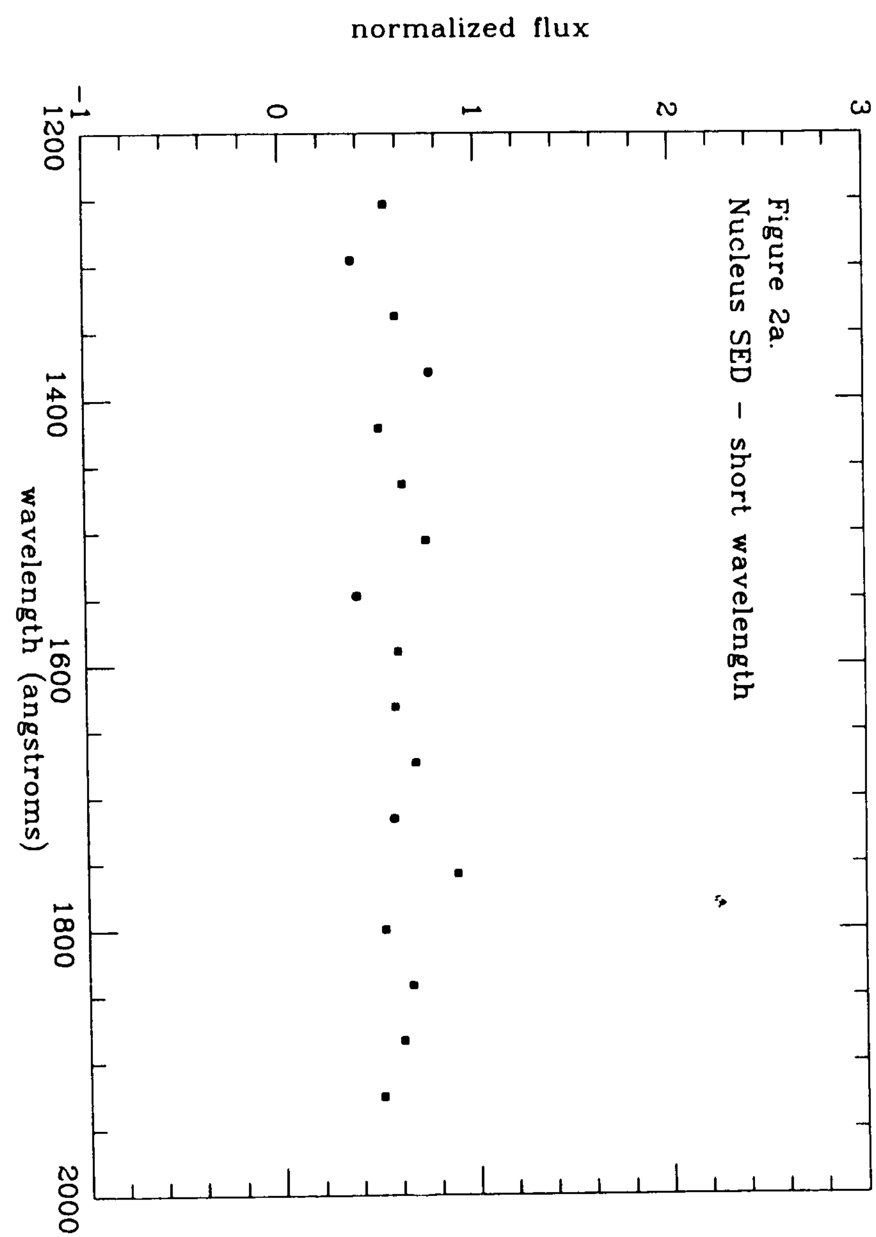

Figure Captions

Figure 1. Photograph of NGC 205

Figure 2. The short and long wavelength SEDs are shown for the Nucleus (2a. and 2b.) and Region B (2c. and 2d.). The intensities have been normalized to $1.0\times10^{-14} ergs^{-1} cm^{-2}$. The short wavelength SEDs have been binned into 35Å bins, while the long wavelength SEDs are binned to 50Å bins.

Figure 3a-b. IUE archive spectrum of 47 Tuc. These spectra have also been normalized to $1.0\times10^{-14} ergs^{-1} cm^{-2}$.

Figure 4a-b. Observed spectra for both the Nucleus and Region B are shown to highlight the spectral features.

Figure 5a-b. Comparison of the Miller-Scalo IMF with two different assumptions concerning the nature of the luminous blue stars (LBS). The solid line shows the integrated spectrum resulting from an IMF assuming the LBS are main sequence stars. The dashed line is the result with assumption that the LBS are evolved giants.

Figure 6a-d. Comparison of the modelled SEDs (filled triangles) with the observed SEDs (filled squares). Parameters of each fit are shown in Table 3.

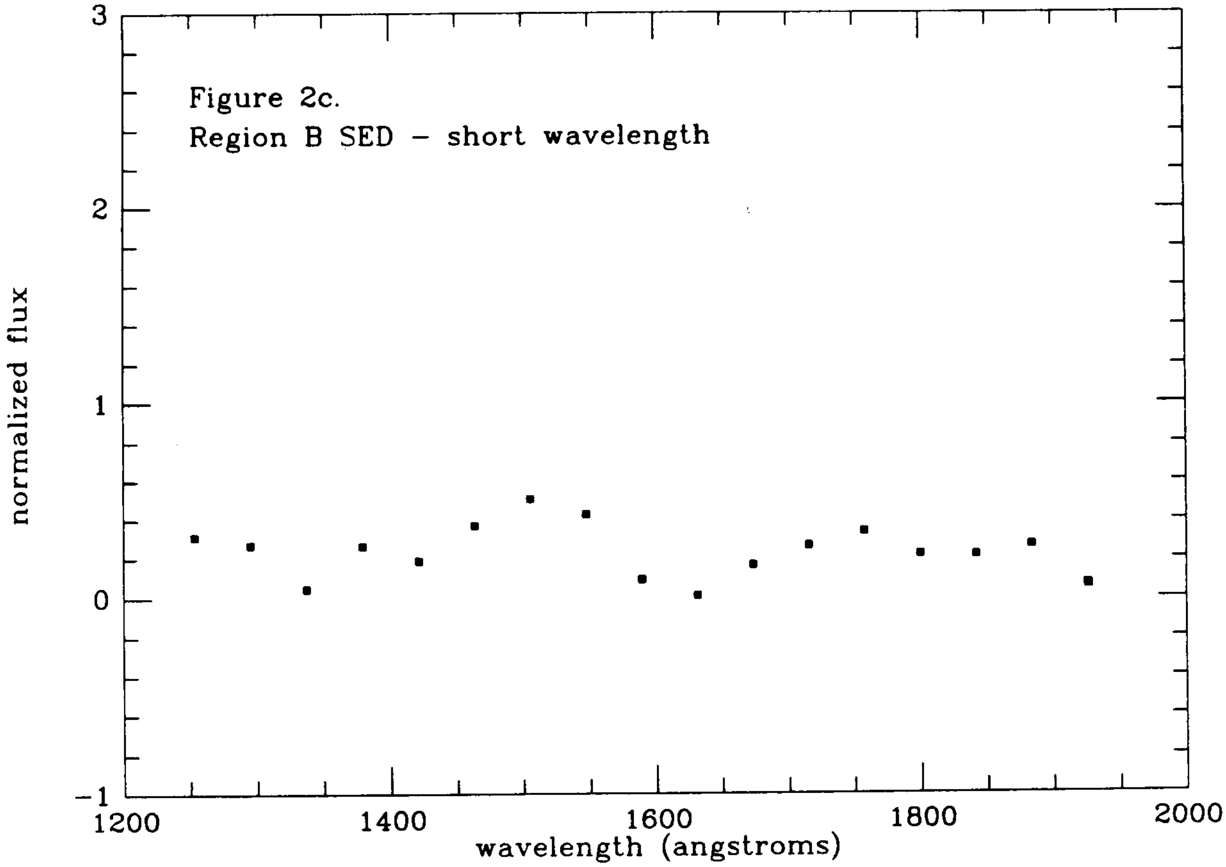
Figure 2c.
Region B SED – short wavelength
normalized flux
wavelength (angstroms)
3
2
1
0
–1
1200
1400
1600
1800
2000

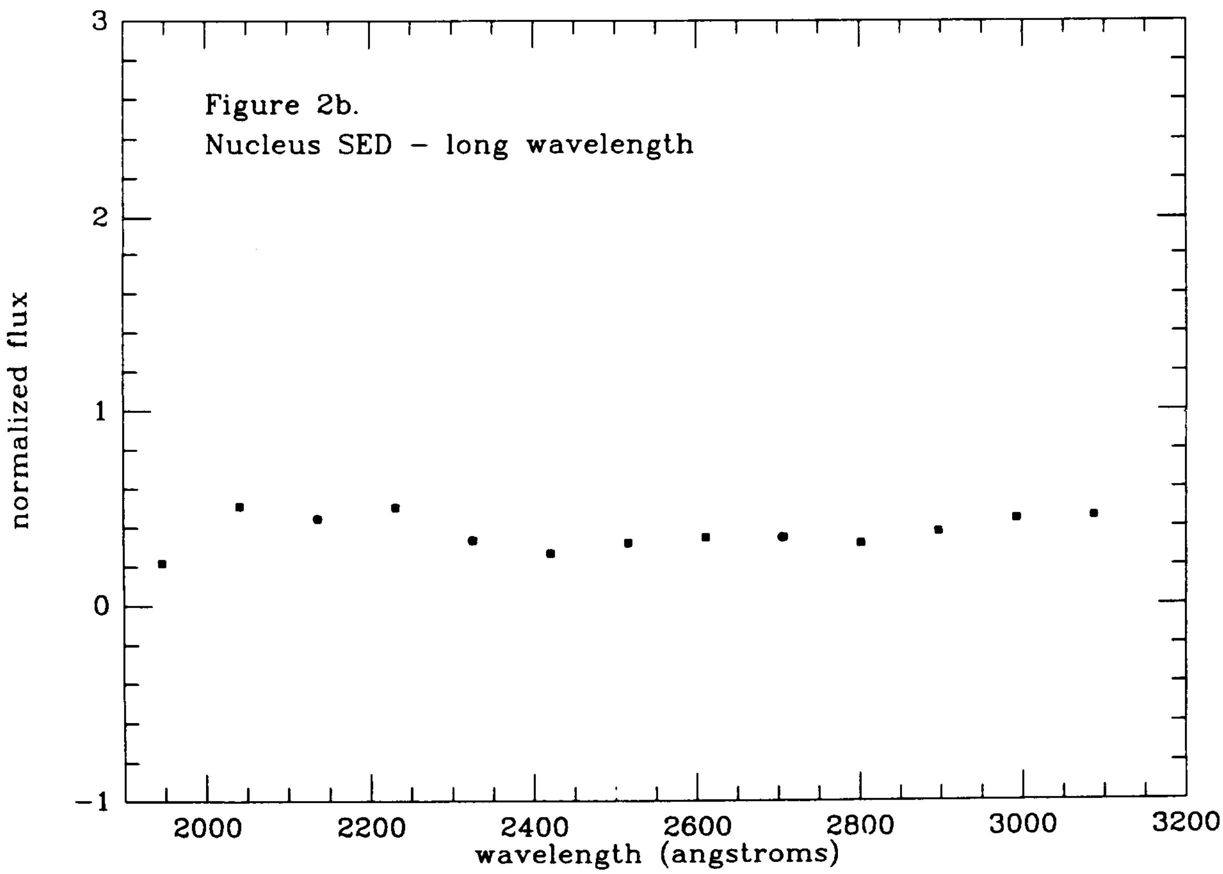
Figure 2b.
Nucleus SED – long wavelength
normalized flux
wavelength (angstroms)
3
2
1
0
–1
2000
2200
2400
2600
2800
3000
3200

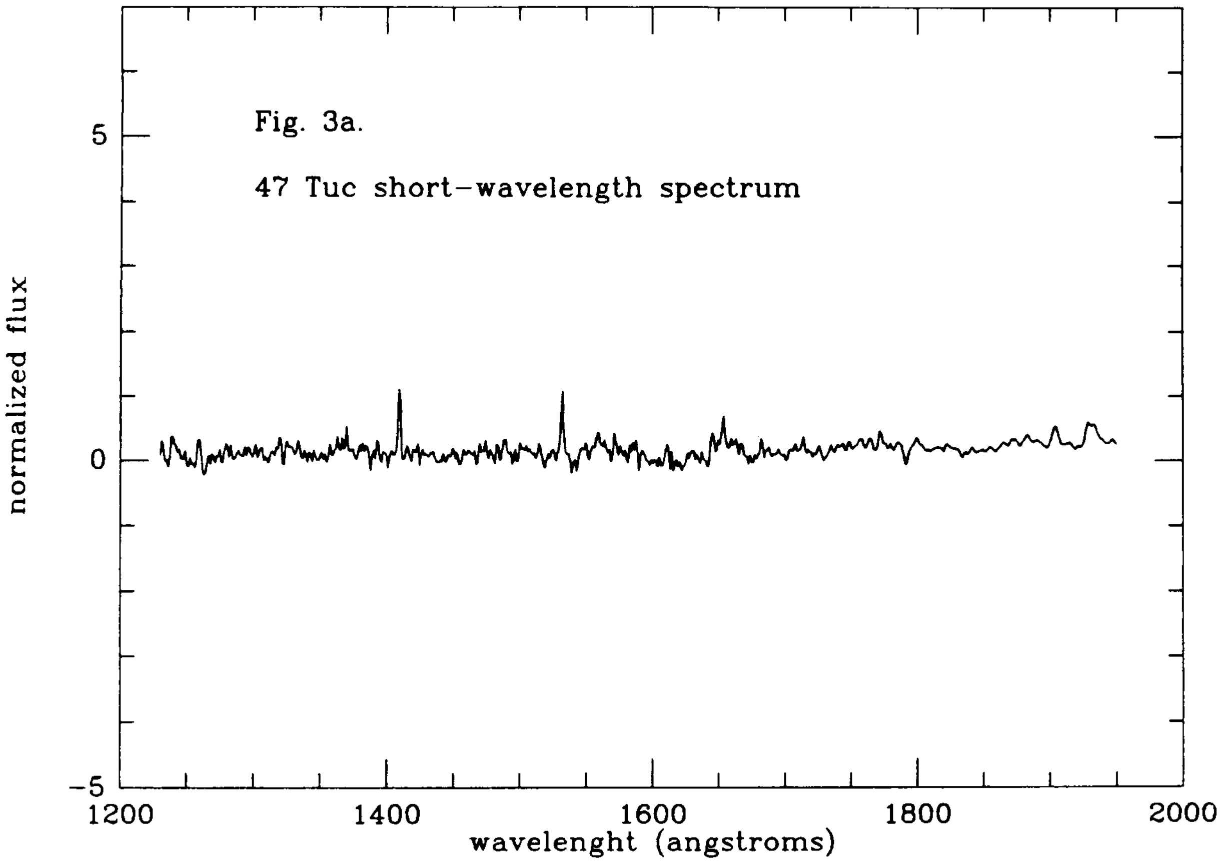
Fig. 3a.
47 Tuc short–wavelength spectrum
normalized flux
5
0
−5
1200
1400
1600
1800
2000
wavelenght (angstroms)

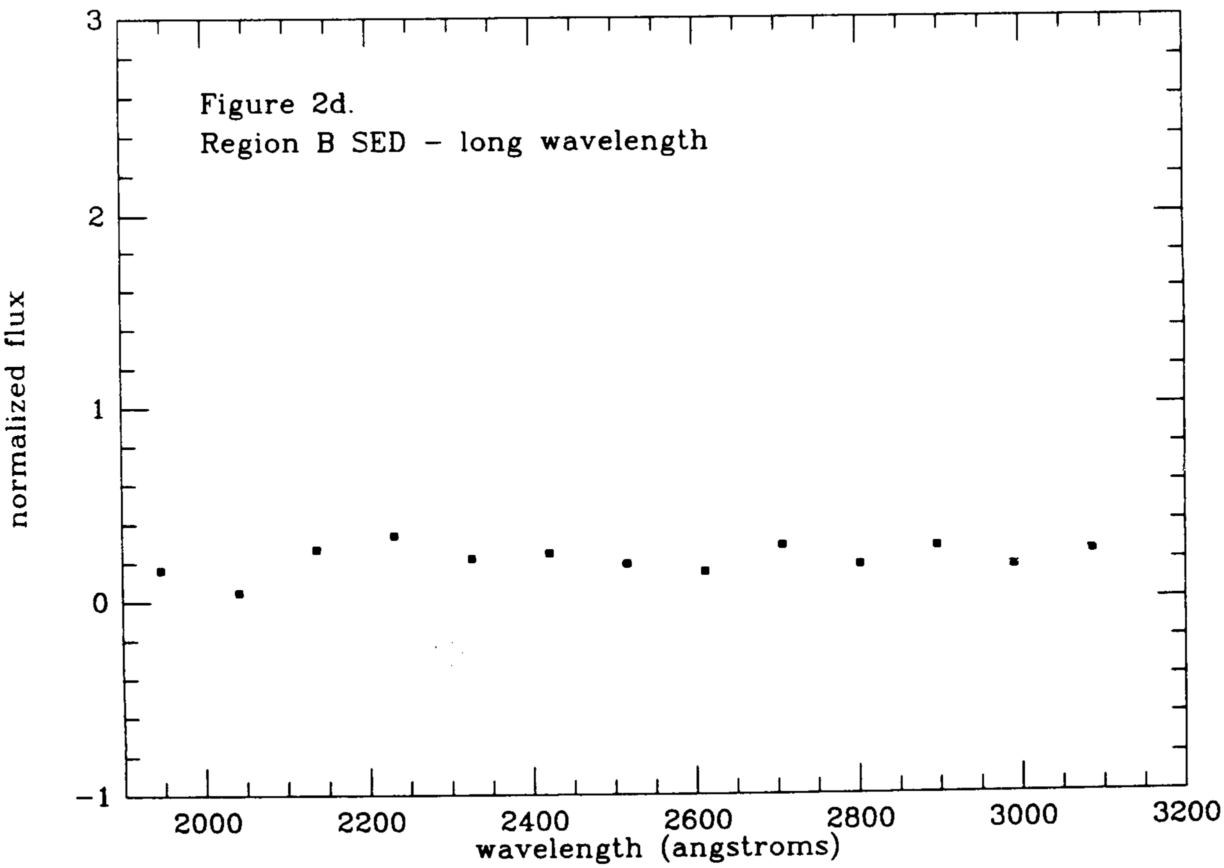
Figure 2d.
Region B SED – long wavelength
normalized flux
3
2
1
0
−1
2000
2200
2400
2600
2800
3000
3200
wavelength (angstroms)

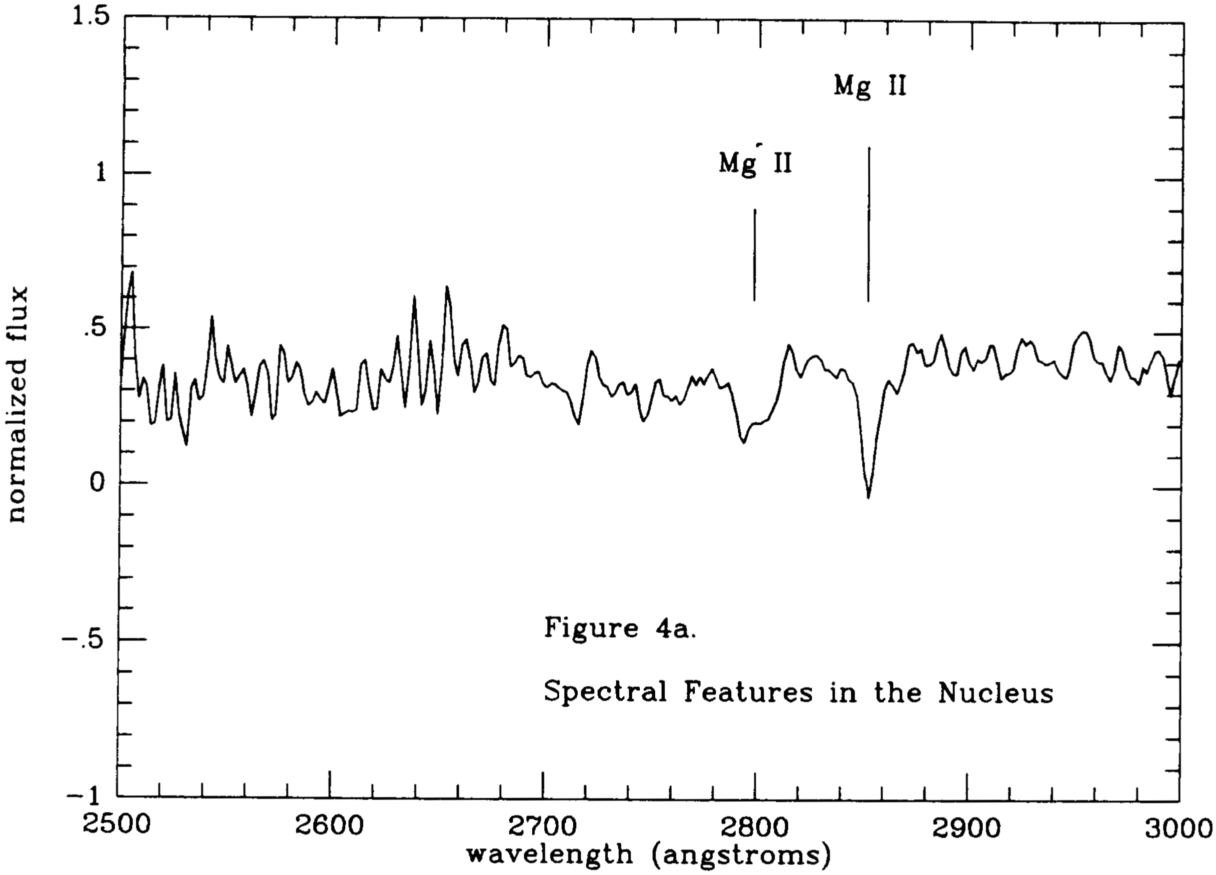

Figure 4a.

Spectral Features in the Nucleus

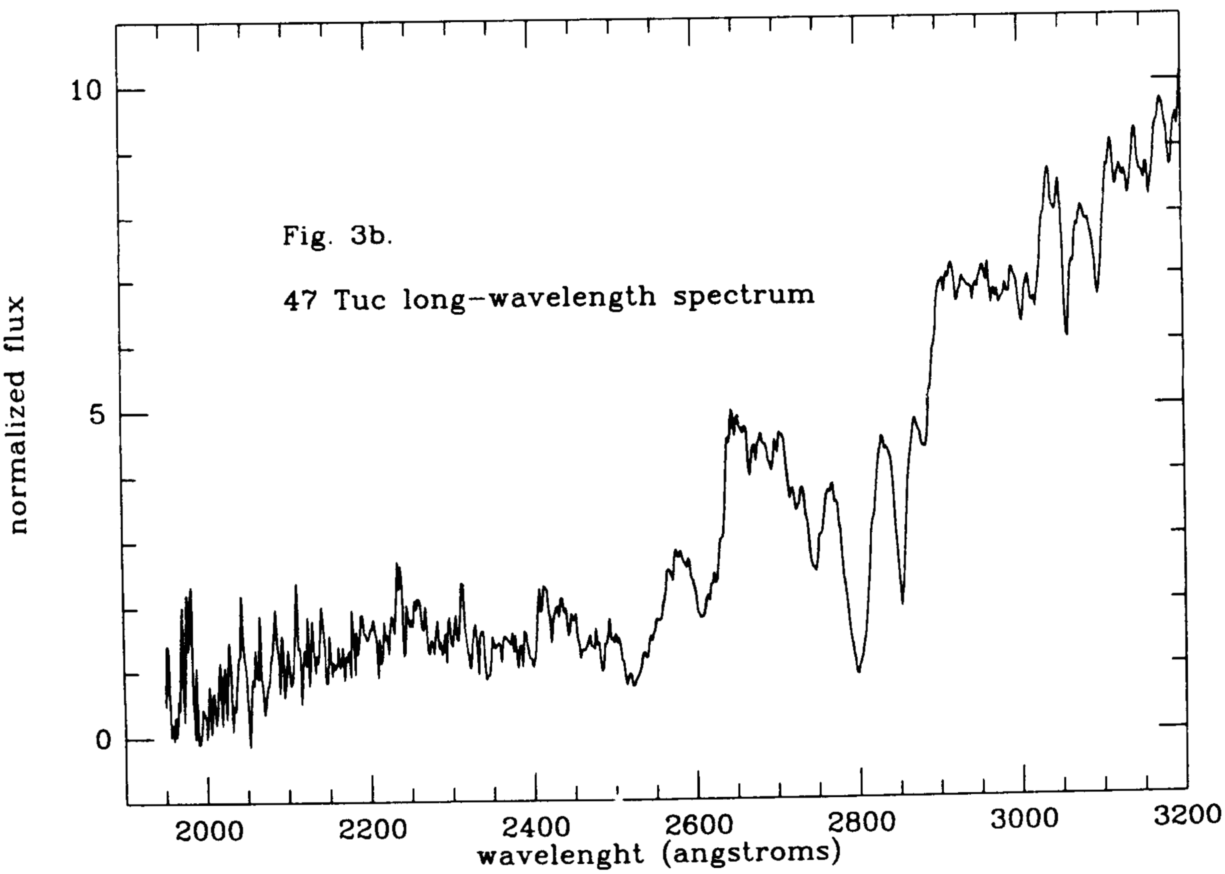

Fig. 3b.

47 Tuc long-wavelength spectrum

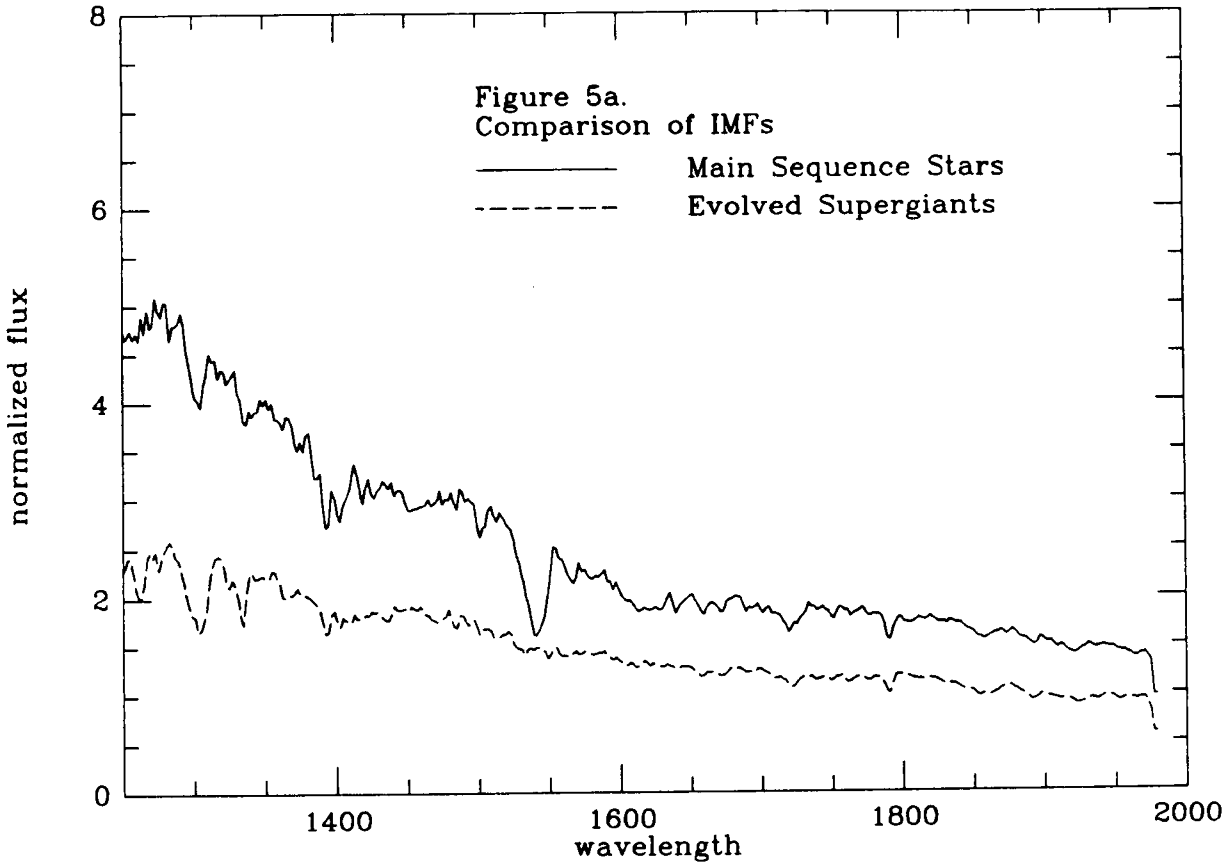

Figure 5a.
Comparison of IMFs
Main Sequence Stars
Evolved Supergiants
normalized flux
wavelength
0
2
4
6
8
1400
1600
1800
2000

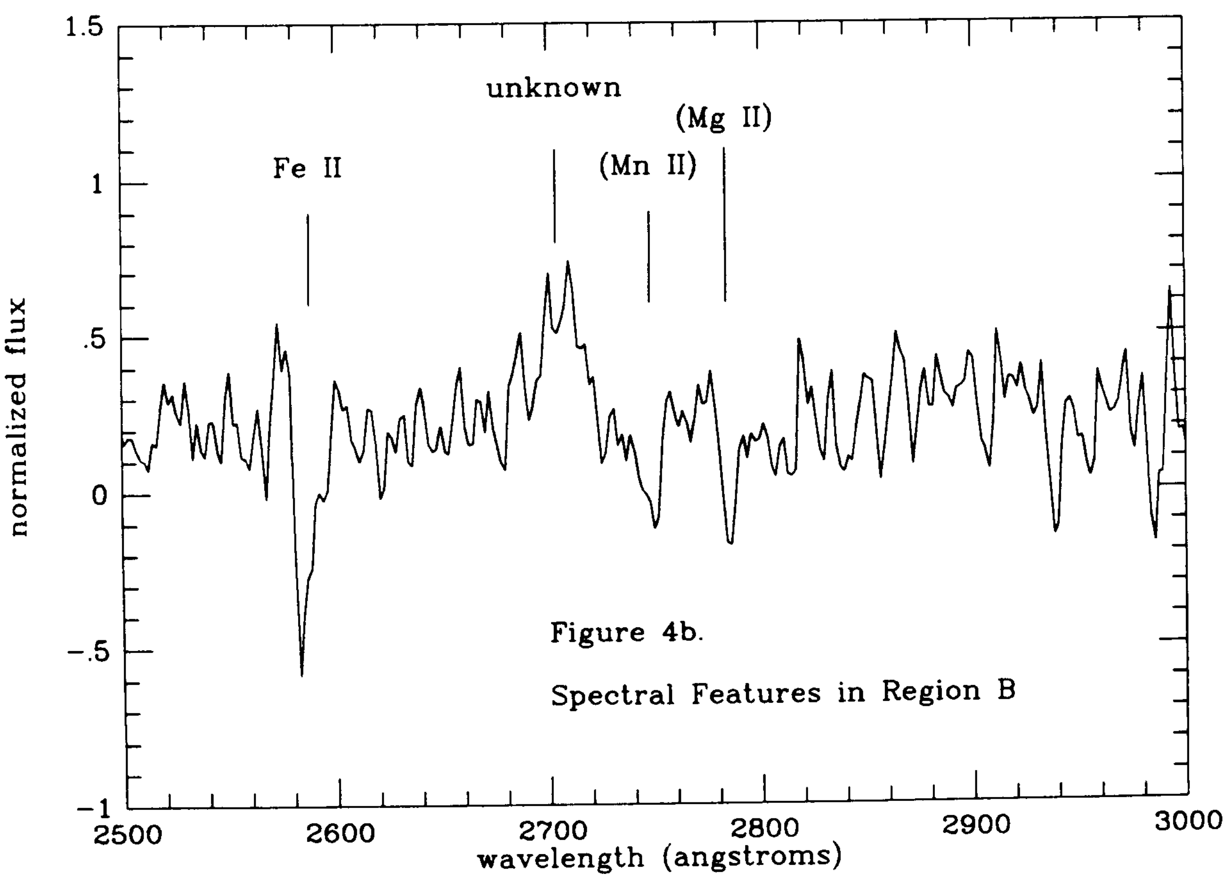

unknown
(Mg II)
Fe II
(Mn II)
Figure 4b.
Spectral Features in Region B
normalized flux
wavelength (angstroms)
1.5
1
.5
0
−.5
−1
2500
2600
2700
2800
2900
3000

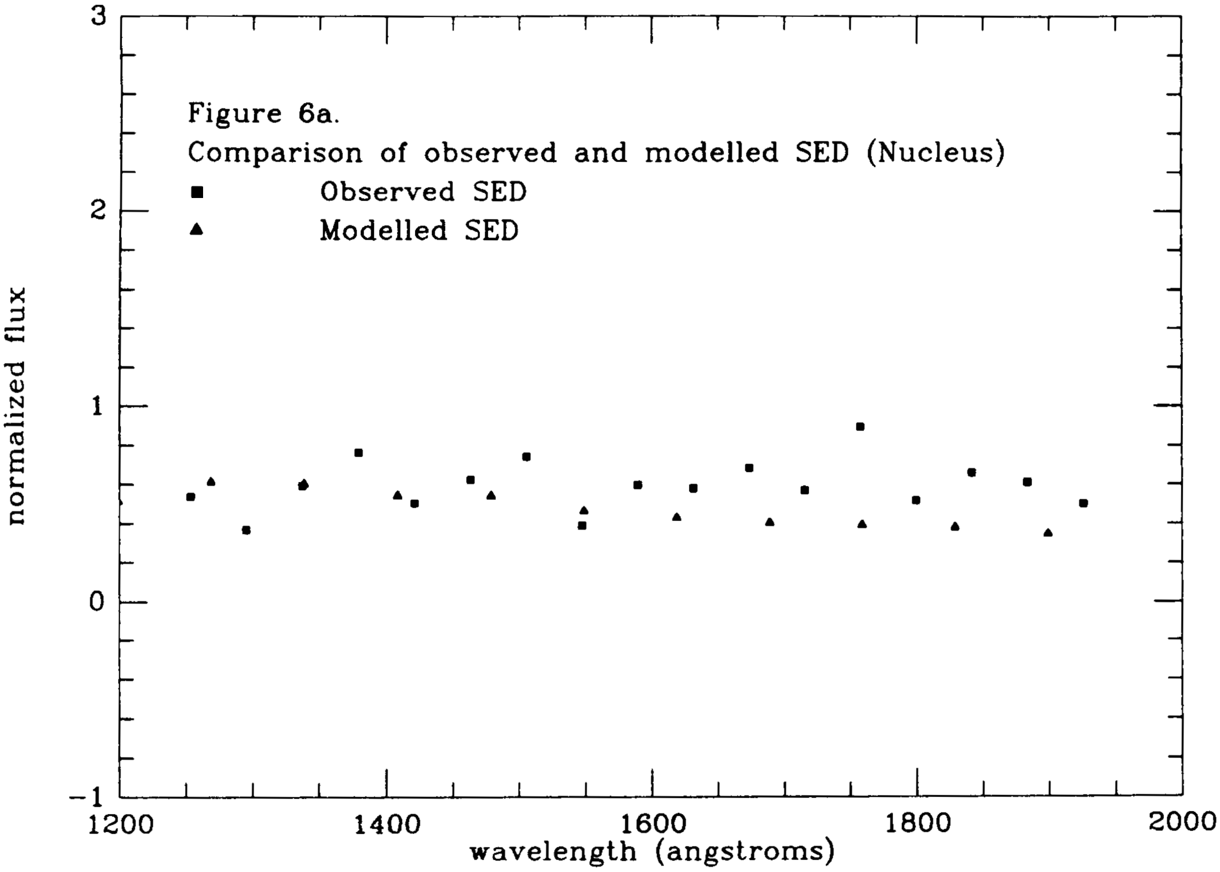
Figure 6a.
Comparison of observed and modelled SED (Nucleus)
Observed SED
Modelled SED
normalized flux
wavelength (angstroms)
3
2
1
0
−1
1200
1400
1600
1800
2000

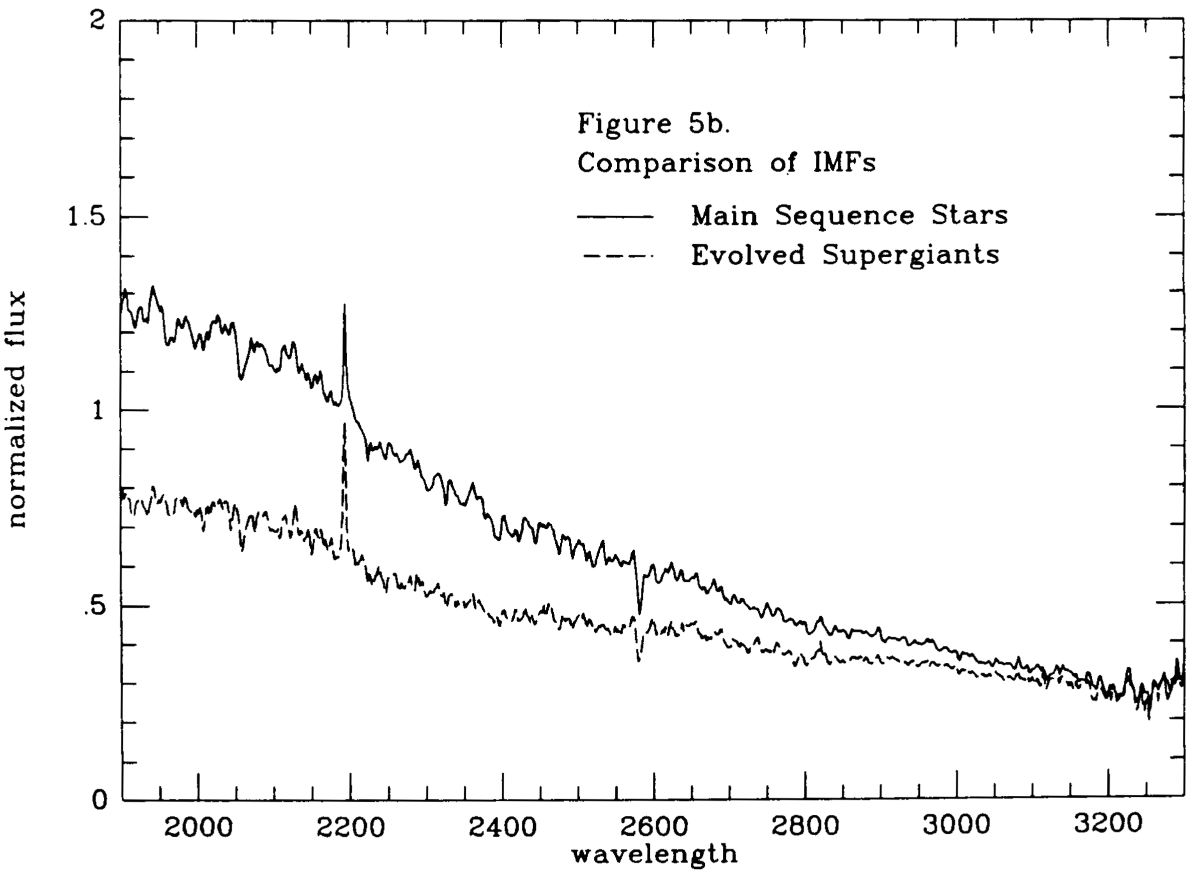
Figure 5b.
Comparison of IMFs
Main Sequence Stars
Evolved Supergiants
normalized flux
wavelength
2
1.5
1
.5
0
2000
2200
2400
2600
2800
3000
3200

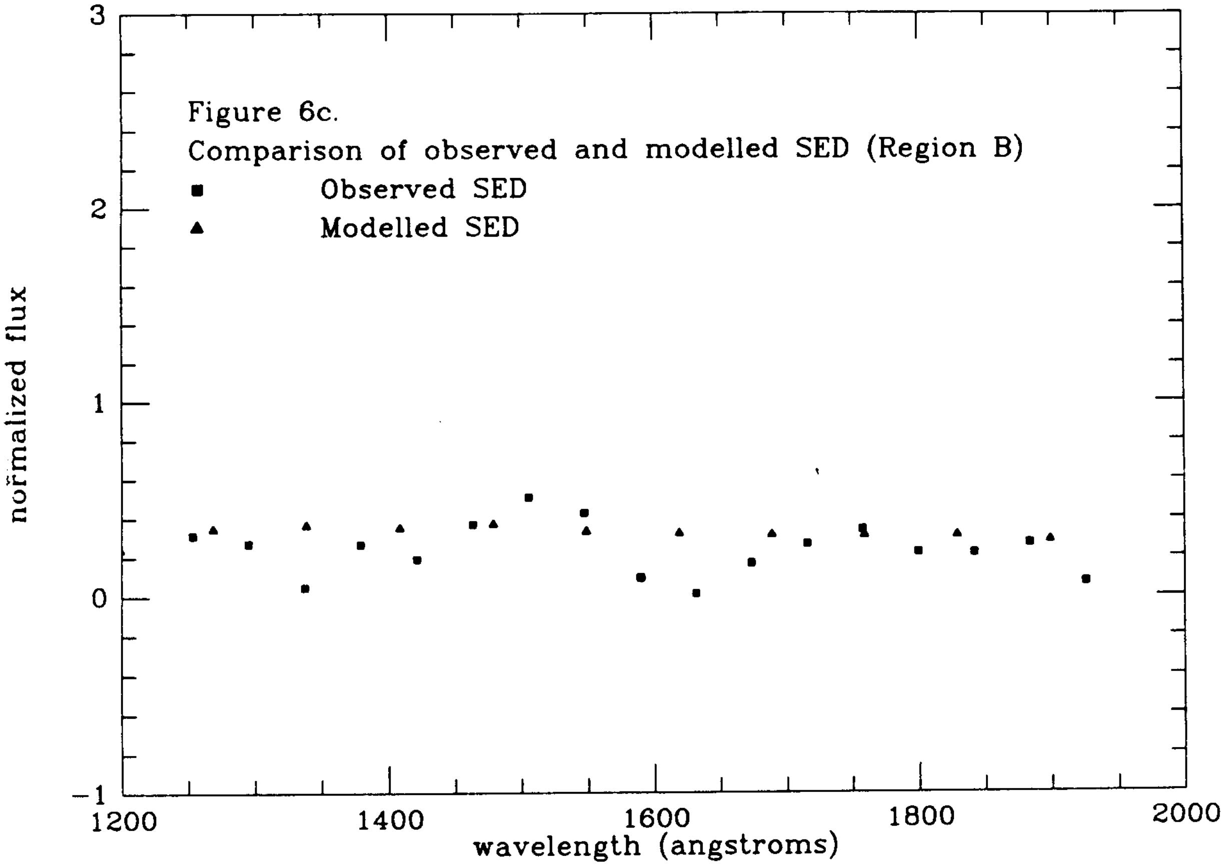
Figure 6c.
Comparison of observed and modelled SED (Region B)
Observed SED
Modelled SED
normalized flux
wavelength (angstroms)
3
2
1
0
−1
1200
1400
1600
1800
2000

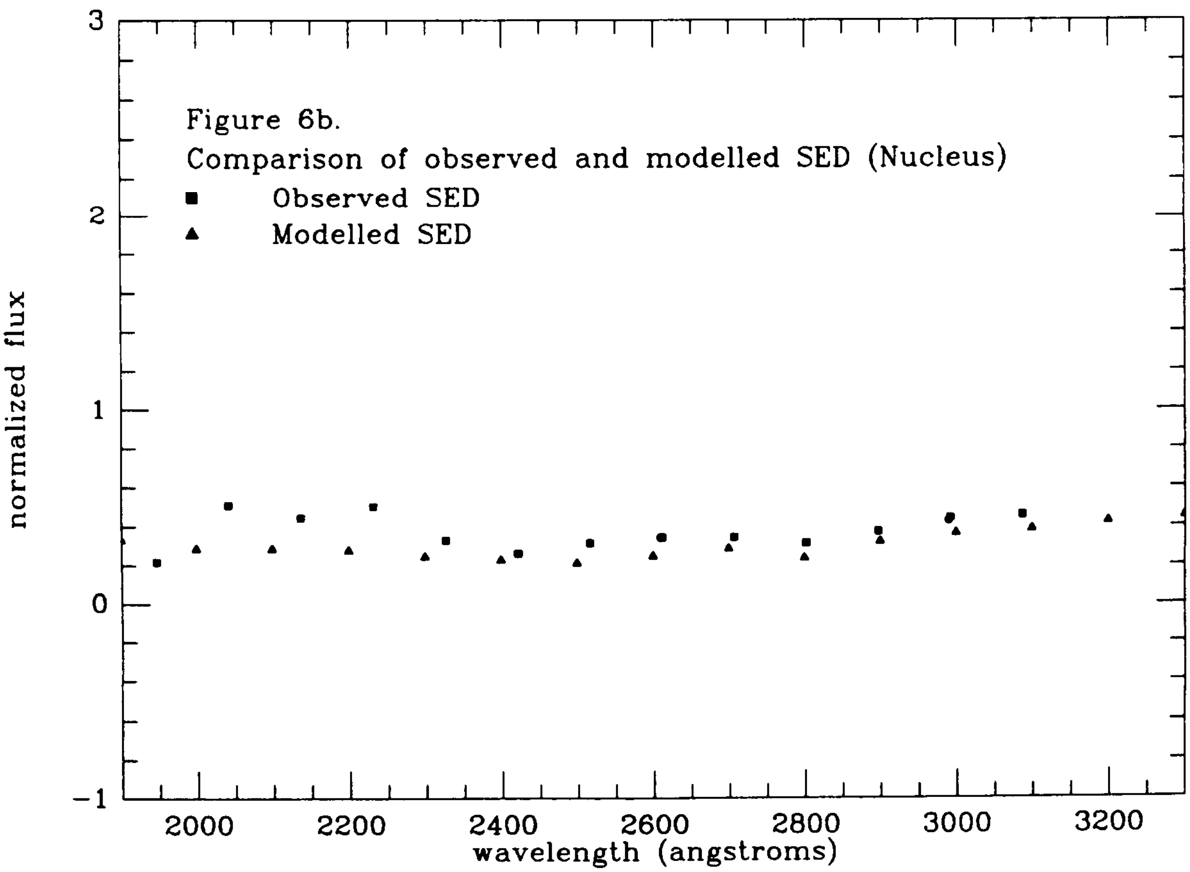
Figure 6b.
Comparison of observed and modelled SED (Nucleus)
Observed SED
Modelled SED
normalized flux
wavelength (angstroms)
3
2
1
0
−1
2000
2200
2400
2600
2800
3000
3200

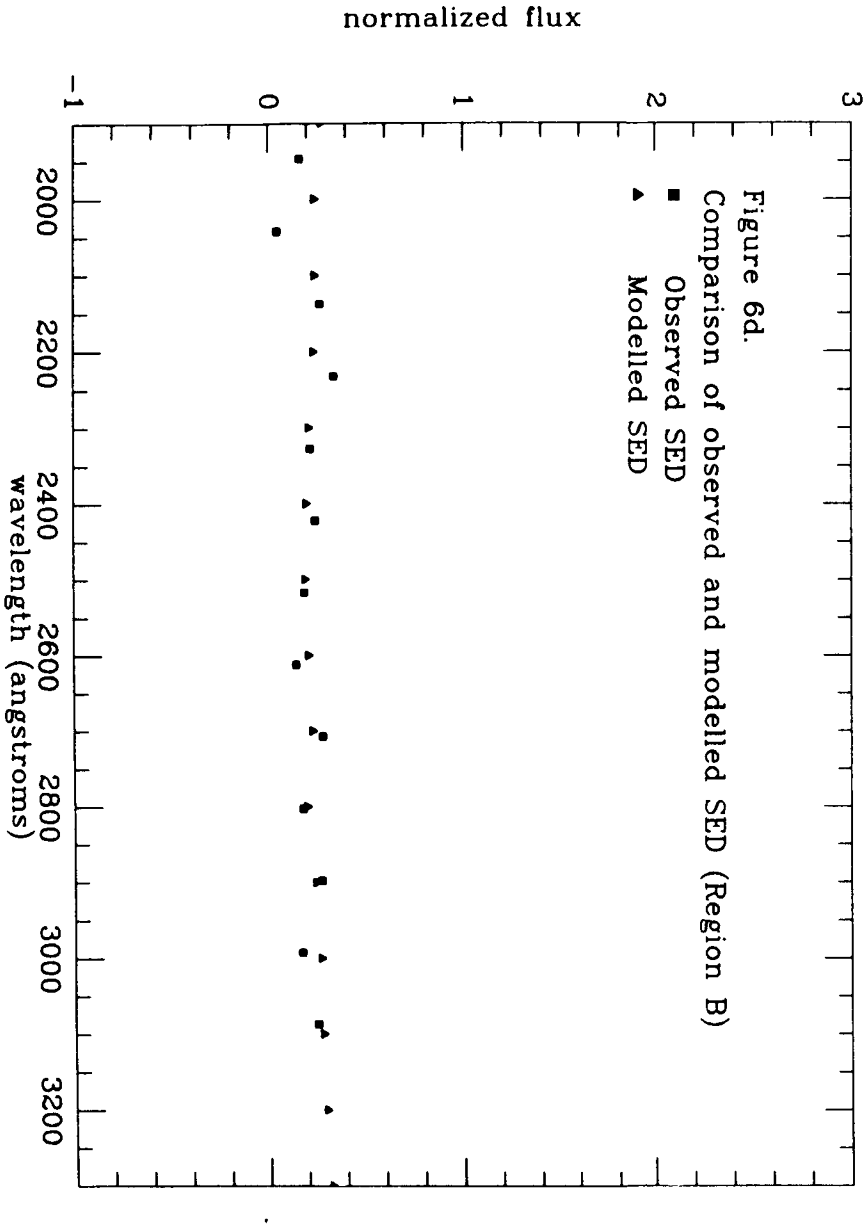

Figure 6d.
Comparison of observed and modelled SED (Region B)

References

Baade, W. 1951, *Pub. Univ. Mich. Obs.*, **10**, 7.

Bertelli, G., Chiosi, C., and Bertola, F. 1989. *Ap. J.*, **339**, 889.

Böhm-Vitense, E., Hodge, P., and Boggs, D. 1984. *Ap. J.*, **287**, 825.

Bruzual, G.A. 1983. *Ap. J.*, **273**, 205.

Burstein, D., and Heiles, C. 1982. *A. J.*, **87**, 1165.

Burstein, D., Bertola, F., Buson, L.M., Faber, S., and Lauer, T.R. 1988, *Ap. J.*, **328**, 440.

Cardelli, J., and Böhm-Vitense, E. 1982. *Ap. J.*, **262**, 213.

Fanelli, M.N., O'Connell, R.W., and Thuan, T.X. 1987, *Ap. J.*, **321**, 768.

Fanelli, M.N., O'Connell, R.W., and Thuan, T.X. 1988, *Ap. J.*, **334**, 665.

Fitzpatrick, E.L., and Savage, B.D. 1982, Wisconsin Astrophysics Preprint, *No.* 158.

Gallagher, J.S., and Mould, J.R. 1981, *Ap. J. Letters*, **244**, L3.

Harris, W.E., and Racine, R. 1979, *Ann. Rev. Astr. Ap.*, **17**, 241.

Hesser, J.E., Harris, W.E., Vandenberg, D.A., Allwright, J.W.B., Shott, P., Stetson, P.B. 1987. *P.A.S.P.*, **99**, 739.

Hodge, P.W. 1973a, *Ap. J.*, **182**, 671.

Hodge, P.W. 1973b, *P.A.S.P.*, **85**, 286.

Humphreys, R.M. 1979a, *AP. J.*, **228**, 364.

Humphreys, R.M. 1979b, *Ap. J. Suppl.*, **39**, 389.

Illingworth, G., and Illingworth, W. 1976. *Ap. J. Suppl.*, **30**, 227.

Johnson, D.W., and Gottesman, S.T. 1983. *Ap. J.*, **275**, 549.

Kennicutt, R.C. 1989, *Ap. J.*, **344**, 685.

Kormendy, J. 1985, *Ap. J.*, **295**, 73.

Maeder, A., and Meynet, G. 1987, *Astr. Ap.*, **182**, 243.

Massey, P., Parker, J.W., and Garmany, C.D. 1989, *A. J.*, **98**, 1305.

Mathis, J.S. 1987, *in Exploring the Universe with the IUE Satellite*, Kondo *et. al* eds., 517.

Miller, G., and Scalo, J. 1979, *Ap. J. Suppl.*, **41**, 513.

Mould, J., Kristian, J., and DaCosta, G. 1984, *Ap. J.*, **278**, 575.

Nandy, K. 1984, *in Structure and Evolution of the Magellanic Clouds*, van den Bergh, S., and de Boer, K.S. eds., 341.

Nesci, R. 1981, *Astr. Ap.*, **99**, 120.

Nesci, R., and Perola, G.C. 1985, *Astr. Ap.*, **145**, 296.

Pickles, A.J. 1985, *Ap. J.*, **296**, 340.

Price, J.S., and Grasdalen, G.L. 1983, *Ap. J.*, **275**, 559.

Richer, H., Crabtree, D., and Pritchet, C.J. 1984, *Ap. J.*, **287**, 138.

Salpeter, E.E. 1955, *Ap. J.*, **121**, 161.

Savage, B.D., and Mathis, J.S. 1979, *Ann. Rev. Astr. Ap.*, **17**, 73.

Seaton, M.J. 1979, *M.N.R.A.S.*, **187**, 73p.

Wu, C.C., Ake, T.B., Boggess, A., Bohlin, R.C., Imhoff, C.L., Holm, A.V., Levay, Z.G., Panek, R.J., Schiffer, F.H., Turnrose, B.E. 1983, IUE NASA Newsletter, No. 22.

Eric M. Wilcots, Paul W. Hodge, and Erika Böhm-Vitense
Department of Astronomy, FM-20
University of Washington Seattle, WA 98195
Paul B. Eskridge
Physics Department
Rensselaer Polytechnic Institute Troy, NY 12180
Francesco Bertola
Dipartimento di Astronomia, Vicolo dell'Osservatorio 5, 35122
Padova, Italy